Journal of Materials Chemistry A

Accepted Manuscript

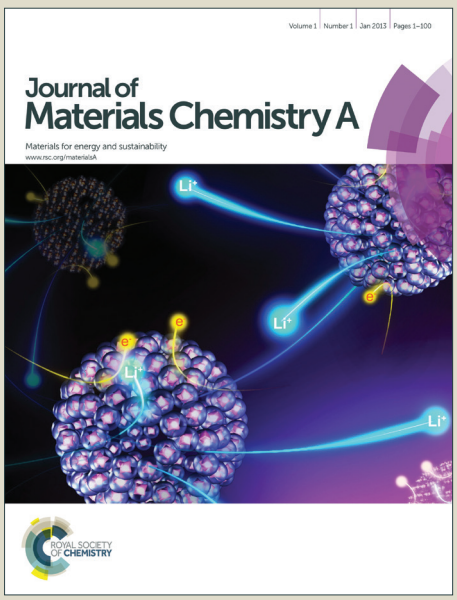

ROYAL SOCIETY OF CHEMISTRY

www.rsc.org/materialsA

Table of contents

Title: Pyrene-conjugated Porphyrins for Efficient Mesoscopic Solar Cells: the role of spacer
Authors: J. Lu, S. Liu, H. Li, Y. Shen, J. Xu, Y. Cheng, and M. Wang

Pyrene-conjugated porphyrin dyes with various π-spacers between the porphyrin chromophore and carboxylic acid have been designed and synthesized in this study, showing an overall power conversion efficiency of 8.7% under full sunlight (AM 1.5G, 100 mW cm^{-2}) irradiation.

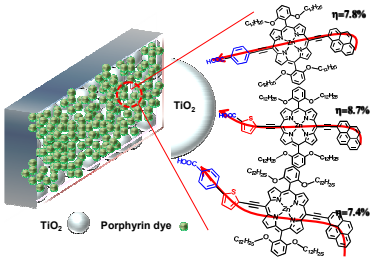

Cite this: DOI: 10.1039/c0xx00000x

www.rsc.org/xxxxxx

ARTICLE TYPE

Pyrene-conjugated Porphyrins for Efficient Mesoscopic Solar Cells: the role of spacer

Jianfeng Lu[‡ a], Shuangshuang Liu[‡ a], Hao Li [a], Yan Shen [a], Jie Xu*[b], Yibing Cheng [a,c], and Mingkui Wang*[a]

Received (in XXX, XXX) Xth XXXXXXXXX 20XX, Accepted Xth XXXXXXXXX 20XX
DOI: 10.1039/b000000x.

With the view of broadening porphyrin light-harvesting cross section and improving mesoporous solar cells power conversion efficiency, pyrene-conjugated porphyrin dyes with various π-spacers between the porphyrin chromophore and carboxylic acid have been designed and synthesized in this study, including the tailors with phenyl (LW17), thiophene (LW18), and 2-phenylthiophene (LW19). These novel porphyrins show stepwise red-shifted absorption spectra and consistently decreased oxidation potential when the spacer changes from phenyl to an electron-rich unit of thiophene, and an elongated spacer of 2-phenylthiophene for LW17, LW18, and LW19 dyes. The mesoporous solar cell based on LW18 dye can achieve an overall power conversion efficiency of 8.7% under full sunlight (AM 1.5G, 100 mW cm^{-2}) irradiation. The result reveals that both photocurrent and photovoltage can be effectively tuned by changing the spacers. Detailed investigation with transient photovoltage decay measurement provides general information on factors affecting the principal photovoltaic parameters.

Introduction

Dye–sensitized solar cells (DSSCs) attracted considerable attention due to their advantages including low cost, ease fabrication, and modifiable aesthetic features of color and transparency.[1] Initial forms of this technology employed ruthenium complex sensitizers achieving a certified solar-to-electric power conversion efficiency (PCE) of more than 11%.[2] However, the relatively high cost and environmental issues of ruthenium complexes encouraged search for noble-metal-free light-harvesters.[3] Porphyrins are particularly promising sensitizers in DSSCs due to their structural similarity to chlorophylls in natural photosynthetic systems as well as their strong and tunable absorption properties. These properties lead to potential application of porphyrins in several areas, including optoelectronics, chemosensors, and catalysis.[4] New benchmark in DSSCs with overall PCE of 13.0% was achieved by a donor-π-acceptor (D-π-A) porphyrin (SM315) with cobalt redox couple.[5]

Typical porphyrins present poor light-harvesting capability at wavelengths around 500 nm and beyond 700 nm.[6] Fortunately, their absorption spectra can be red-shifted and broadened by elongating of π-conjugation as well as enhancing of push-pull character in porphyrins.[6] For example, Yeh, Lin and Diau *et al.* have proposaled a new family of efficient sensitizers (D-π-A style) featuring with using a zinc porphyrin chromophore as π bridge as well as donor and acceptor moieties at the *meso*-position. This creates a judicious directional electron flow from donor to acceptor moiety upon photoexciting.[7] In this case, the effects of electron-donating substituent attached to porphyrin chromophore have been addressed extensively,[8] in which pyrene-conjugated porphyrins was demonstrated to be efficient donor and π-conjugation moieties. Highly effeicient DSSC devices with over 10% PCE were achieved by incorporating 4-ethynylbenzoic acid as acceptor.[9] Meanwhile, it was found that by increasing the electron density of the anchoring group, one can lower down molecule's LUMO energy levels, and extend the light-harvesting area of the dye.[10] For instance, oligomerthiophene, 2,3,5,6-tetra-fluorophenyl, diketopyrrolo-pyrrole, and other functional groups were sucsessfully employed as π-spacer between porphyrin chromophore and anchoring group (carboxylic acid or cyanoacetic acid).[11] Several investigation indicated they posses an extended light-harvesting cross section, and therefore, an improved device efficiency comparsion with sensitizers with 4-ethynylbenzoic acid acceptor.[11] More recently, Grätzel *et al.* reengineered the prototypical structure of D–π–A porphyrins' acceptor by inserting an electron-deficient unit benzothiadiazole (BTD) between the porphyrin chromophore and benzoic acid, affording senstitizers with an broadened absorption spectra.[12] Highly efficiency of 13% was achieved with the porphyrin SM315, which was superior than porphyrin SM371 with benzoic acid as acceptor. While the BTD was inserted directly between the porphyrin chromophore and carboxylic acid, the corresponding DSSC was observed with an decreased PCE. In our previous study, the incident photon to current efficiency (IPCE) response of DSSCs was extended up to 850 nm by inserting electron-rich unit (such as thiophene, EDOT, CPDT) between porphyrin chromophore and cyanoacetic acid.[13] Unfotunately, a decreased photovoltage was oberved which could

be ascribed to an increased recombination accelarted by cyanoacetic acid anchoring group. This result could be also attributed to the H–aggregation of porphyrin dyes with a rotary cyanoacetic acid on the TiO_2 nanoparticles. Similar phenomenon was observed by Bisquert and Diau as well.[14]

As discussed above, a rigid molecular structure is essential for D–π–A porphyrins to reduce charge recombination at the dye–sensitized TiO_2/electrolyte interface.[15] According to Marcus theory, the electronic coupling between donor and acceptor decreases exponentially with increasing the distance between them.[16] Charge separation and electron injection after photoexcitation can be affected by tunning π–spacer. Therefore, π-spacer between porphyrin chromophore and anchoring group becomes one of the key issues in designing of new pigments in order to further improve porphyrin-based DSSC devices efficiency.

Herein we report on an experimental investigation of porphyrin dyes by varying the spacer between porphyrin chromophore and carboxylic acid with the view of broadening the light-harvesting area, and eventually improving the DSSCs performance.[17] Based on the prototypical structure of pyrene-porphyrin conjugate as donor and π-conjugation moieties, phenyl, thiophene, and 2-phenyl-thiophene were selected as spacer to construct porphyrin dyes LW17, LW18, and LW19, respectively. LW19 dye is similar to the famous GY50 dye while the electron-deficient unit BTD is switched with an electron-rich unit thiophene.[12b] LW18 dye is similar to porphyrin GY21.[12] The motivation of our design of D-π-A porphyrin is to investigate the influence of electron-rich unit as spacer on DSSC devices photovaltiac performance. These LW17, LW18 and LW19 dyes showed stepwise red-shifted absorption spectra and decreased oxidation potential when the spacer changes from phenyl to thiophene, and an elongated spacer of 2-phenylthiophene. Time-resolved photoluminescence (TRPL) indicated a similar high hot-electron injection yield. Evaluating the porphyrins with DSSC device, PCE of 8.7% was achieved by LW18 devices under full sunlight (AM 1.5G, 100 mW cm^{-2}) irradiation, while it was 7.8% for LW17 and 7.3% for LW19 devices. Transient photovoltage decay (TPD) measurement was performed to provide detailed influence of π-spacer upon the optoelectronic features of porphyrins dyes in DSSCs.

Results and Discussion

The molecular structure of LW17, LW18, and LW19 porphyrins are presented in Scheme 1. Bearing with the same pyrene-porphyrin conjugates as donor and carboxyl acid as acceptor, the spacer between porphyrin chromophore and carboxylic acid was varied with phenyl, thiophene, and 2–phenylthiophene. Detailed synthetic procedures are described in Scheme 2. The synthetic approach to these ethynyl-bridged porphyrins has been designed on the basis of Sonogashira coupling reaction reported by Lindsey *et al.*[18] The starting reaction between the key precursor of 5,15 dibromo-10,20-bis[2,6-di(dodecyloxy)phenyl] porphyrin zinc(II) (coded as **ZnPBr$_2$**)[19] and 1-ethynylpyrene produced the green intermediate of compound **Por–1**. Then, **Por–1** was reacted with 4–ethynylbenzoic acid, 5–ethynylthiophene-2-carboxylic acid, 4–(5–ethynylthiophen–2–yl)benzoic acid through Sonogashira-Hagihara coupling reaction to obtain LW17, LW18, and LW19 dyes. The structure and purity of all the intermediates and final compounds were identified by NMR, high-resolution mass spectrometry and FTIR (see Figs. S1-S10 in supporting information).

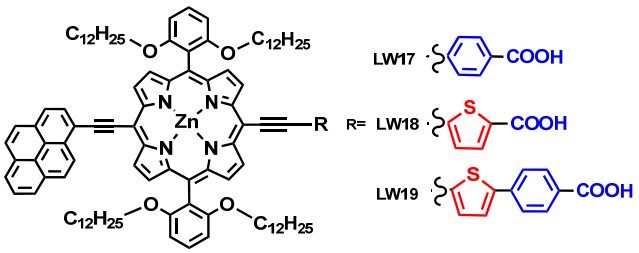

Scheme 1 Molecular Structure of porphyrin sensitizers LW17, LW18, and LW19.

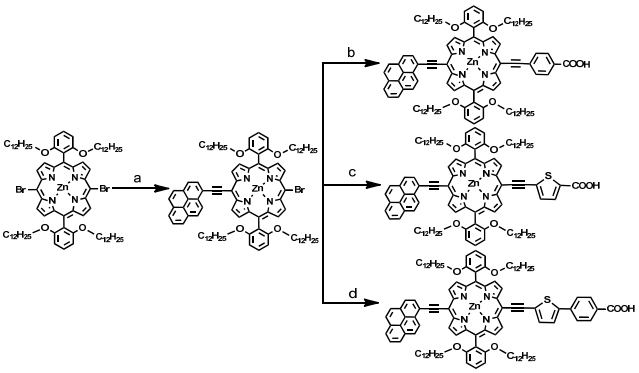

Scheme 2 Synthetic routs for LW17, LW18, and LW19 porphyrins: a) 1-ethynylpyrene, $Pd(PPh_3)_4$, CuI, TEA/THF, 40 °C, 24 h; b) 4-ethynylbenzoic acid, $Pd(PPh_3)_4$, CuI, TEA/THF, 45 °C, 17 h; c) 5-ethynylthiophene-2-carboxylic acid, $Pd(PPh_3)_4$, CuI, TEA/THF, 45 °C, 17 h; d) 4-(5-ethynylthiophen-2-yl)benzoic acid, $Pd(PPh_3)_4$, CuI, TEA/THF, 45 °C, 17 h.

The absorption spectra of LW17, LW18, and LW19 porphyrins in THF is displayed in Fig. 1 and the corresponding data are tabulated in Table 1. In THF solution, LW17, LW18, and LW19 porphyrins exhibited progressive red-shifted absorption spectra. The maximum in the visible region were found at 469, 470, and 474 nm corresponding to their B band, 674, 678 and 683 nm for the Q band, stemming from $S_0 \rightarrow S_2$ transition and $S_0 \rightarrow S_1$ transition, respectively.[20] The absorption band of LW18 porphyrin (thiophene) was toltaly red-shifted compared to LW17 porphyrin (phenyl), indicating a positive effect upon the replacement of phenyl with thiophene. Further red-shifted of the absorption bands were observed in LW19 porphyrin (2-phenylthiophene). The absorption intesity of the B and Q band decreases in the order of LW19<LW18<LW17, accompanying with a gradual red-shift of the B and Q band (LW17<LW18<LW19). The spectral change for these porphyrins can be interpreted by decreasing symmetry and extended π-conjugation. These results are well-consistent with the literature reports.[21]

Fig. S11 compares the absorption spectra of the synthesized porphyrins in THF with those on 2.3 μm TiO_2 films. Only a short dye soaking time (about 2 min) was allowed to avoid a saturation of the B-band absorption. Thus, small amounts of porphyrins were adsorbed onto the TiO_2 films. The B and Q bands of porphyrin-sensitized films were slightly blue shifted and considerably broadened comparing to the solution spectra, indicating a slight H-aggregation of the adsorbed state porphyrins on the TiO_2. The H-aggregation of porphyrins occured when the transition dipole moments of molecules were parallelly aligned ("face-to-face").[22]

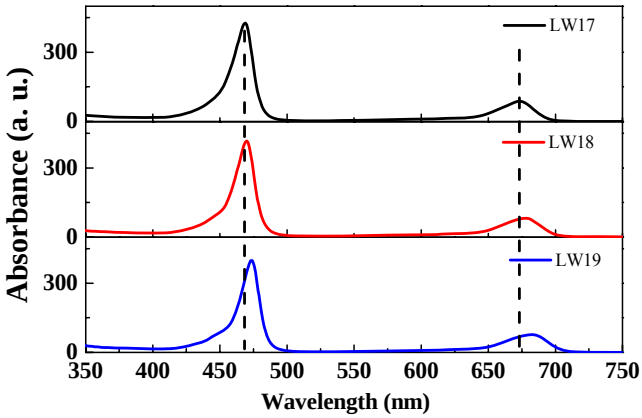

Fig. 1 UV-visible absorption spectra of LW17, LW18, and LW19 porphyrins in THF.

Fig. 2 presents the fluorescence emission spectra of LW17, LW18, and LW19. The major fluorescent emission bands were found at 686, 702, and 725 nm, showing mirror images of their Q bands. The same trend suggests that the various spacers affect porphyrin similarly in both light absorption and emission.

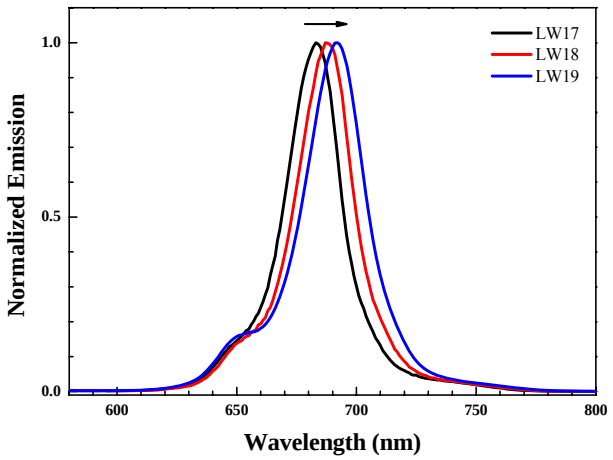

Fig. 2 Normalized PL spectra of LW17, LW18, and LW19 in THF.

The electrochemical behavior of LW17, LW18, and LW19 porphyrins was explored with cyclic voltammetry. The results are presented in Fig. S12 and Table 1. The values of first oxidation potential (Eox) were calaculated to be 0.91, 0.92 to 0.93 V (vs. NHE) for LW17, LW18, and LW19 dyes, indicating a gradually increased HOMO energy levels. The HOMO-LUMO gaps were determined to be 1.83, 1.82, and 1.80 eV for the three dyes respectively, by calculating from the intersection of their absorption and emission spectrum. Thus, the excited state dye energy levels (dye*/dye^+) were estimated to be -0.92, -0.90 and -0.87 V (vs. NHE), respectively. Fig. 3 presents a schematic energy-level diagram of LW17, LW18, and LW19 porphyrins, indicating that efficient dye regeneration and electron injection processes for LW17, LW18, and LW19 dye-sensitized TiO_2 systems are all energetically favorable.[24]

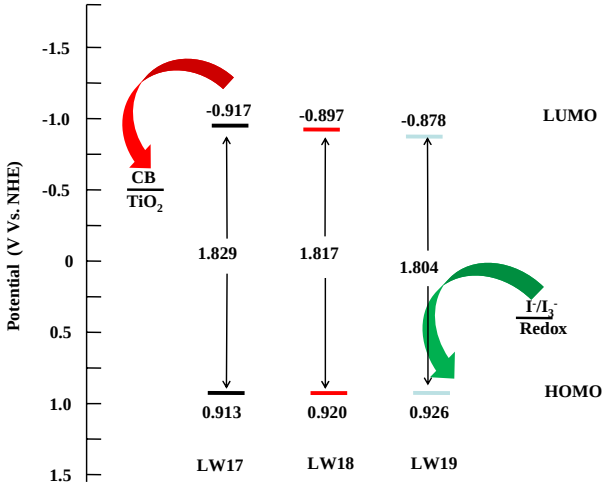

Fig. 3 A schematic energy-level diagram of LW17, LW18, and LW19 porphyrins.

Density functional theory (DFT) at the B3LYP/6-31G level was used to gain insight into the molecular geometry, molecular orbital, and the nature of the electronic transition implied in the different absorption bands.[25] The electronic orbital distributions and the corresponding energy levels are displayed in Fig. 4 and Fig. S13. The synthesized dyes present a similar conformation, showing a planar pyrene-porphyrin conjugation structure with varying acceptors. The two meso-phenyl substituents bearing two dodecoxyl (-$OC_{12}H_{25}$) chains at *ortho*-position of each porphyrin are perpendicular to the planar porphyrin conjugation. This configuration is beneficial for avoiding the steric congestion around the *meso*-positions. The HOMOs of new dyes are delocalized through pyrene and porphyrin macrocycle, while their LUMO levels homogeneously distribute through porphyrin core and carboxylic acid anchoring group. This configration benefits an effectively charge transfer across the compound upon excitation. The calculated absorption spectra shows a first vertical excitation at 585 nm (2.12 eV), 605 nm (2.05 eV), and 611 nm (2.03 eV) for LW17, LW18, and LW19 dyes, respectively. This result is consistent with the trend of the experimental values for the lowest-energy Q-bands at 674 nm (1.84 eV), 678 nm (1.83 eV) and 683 nm (1.82 eV) for the three dyes (see Fig. 1). The dipole moments of LW17, LW18, and LW19 dye were computed at 4.34, 5.79, and 4.79 D. The dipole moment is an indictor of push-pull electronic ability. A small dipole moment value corresponds to a weak push-pull character.[26]

TRPL measurement was performed to investigate electron injection from the photoexcited novel porphyrin dyes to the

semiconducting photoanode. Fig. 5 presents the decay plots of LW17, LW18, and LW19 dyes in THF solution and the sensitized

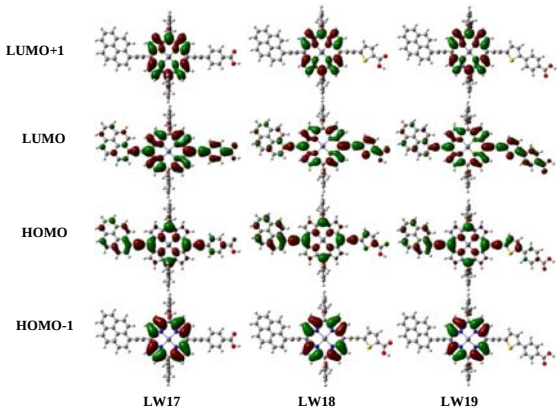

Fig. 4 Isodensity plots of the electronic distributions of the occupied/unoccupied orbitals of LW17, LW18, and LW19 porphyrins computed by a DFT approach using THF solution.

nanocrystalline TiO_2 films filled with electrolytes used in the photovoltaic experiment. The TRPL decay action of these porphyrins are extremely similar, which can be ascribed to the similar structure of molecules except of spacer. By considering the re-convolution of instrument response function, the fluorescence lifetimes for LW17, LW18, and LW19 porphyrins in THF were evaluated to be 1.325, 1.193 and 0.945 ns, respectively. LW18 and LW19 porphyrins present shorter fluorescence lifetime than LW17, which may be attributed to the twisted molecular structure of the former two dyes posessing a thiophene in spacer. When the dyes adsorbed onto TiO_2 nanoparticle surface, strong quenching of the emission was observed as depicted in Fig. 5. The lifetimes of the excited singlet state of LW17, LW18, and LW19 porphyrins of the adsorbed state were estimated to be 44, 68 and 55 ps, respectively. The accelerated emission decay profiles of the novel porphyrins suggests that electron transfer from the excited state of dyes to semiconductors is absolutely fast and efficient.

Table 1 Absorption, fluorescence, and first porphyrin-ring redox potential of various porphyrins (LW17, LW18, and LW19) in THF.

Dye	Absorption [a] λ max (nm 10^3 M^{-1} cm^{-1})	Emission [b] λ max (nm)	PL lifetime [c] (ns)	Eox[d] (V vs. NHE)	$E_{0\text{-}0}$[e] (V vs. NHE)	E_{ox}-$E_{o\text{-}o}$ (eV)
LW 17	469(426.4); 674(87.2)	683	1.325 (0.044)	-0.917	1.829	0.913
LW 18	470(417.2) 678(82.4)	687	1.193 (0.068)	-0.897	1.817	0.920
LW 19	474(398.4) 683(77.4)	692	0.945 (0.055)	-0.878	1.804	0.926

[a] Absorption and emission data were measured in THF at 25 °C Electrochemical measurements were performed at 25 °C with each porphyrin (0.5 mM) in THF/0.1 M TBAP/N_2, GC working and Pt counter electrodes, Ag/AgCl reference electrode, scan rate=50 mV s^{-1}; [b] Excitation wavelength /nm: LW17, 469; LW18, 470; LW19, 474 nm; [c] the fluorescence lifetime were measured under a laser excitation of 445 nm; [d] First porphyrin ring oxidation; [e] Estimated from the intersection wavelengths of the normalized UV-visible absorption and the fluorescence spectra.

The newly synthesized porphyrins were evaluated with DSSCs. By using an optimized binary solvent system of toluene and ethanol (volume ratio 1:1), the porphyrins were adsorped onto a bilayer (7.5 + 5.0 μm) titania film to serve as a working electrode. The photovoltaic parameters, *i.e.*, PCE, short-circuit photocurrent density (J_{SC}), the open-circuit photo-voltage (V_{OC}), and fill factor

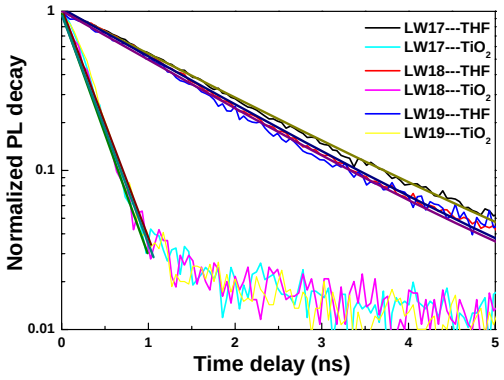

Fig. 5 Time-resolved photoluminescence (TRPL) decay traces of dye-grafted mesoporous titania film and dye in THF solvent. Excitation wavelength: 445 nm.

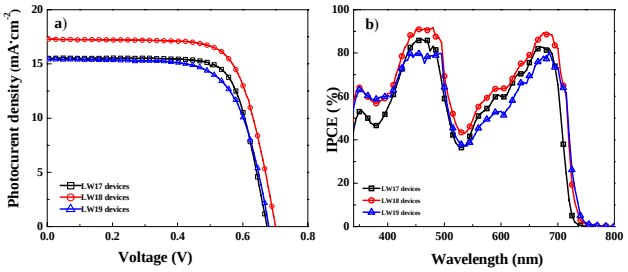

Fig. 6 a) *J-V* curves of and the DSSC devices based on LW17, LW18 and LW19 porphyrins measured under simulated AM 1.5G full-sunlight and b) IPCE spectra of LW17, LW18 and LW19 devices. The cells were measured with a mask (area= 0.09 cm^{-2}).

(*FF*) of LW17, LW18, and LW19 are summarized in Table 2. The *J-V* curves and IPCE spectra are displayed in Fig. 6. The device of LW18 (thiophene) exhibited a J_{SC} of 17.27±0.26 mA cm^{-2}, a V_{OC} of 700±6 mV and a *FF* of 0.71±0.02, giving an superior overall PCE of 8.74±0.22%, while it was 15.67±0.22 mA cm^{-2}, 688±10 mV, 0.72±0.02, 7.81±0.28% for LW17 (phenyl) and 15.42±0.16 mA cm^{-2}, 680±4 mV, 0.68±0.02, 7.26±0.16% for LW19 (2-phenylthiophene) under full sunlight (AM 1.5G, 100 mW cm^{-2}) irradiation. For comparison, the reference porphyrin LD14 gave a PCE of 9.01% under similar conditions. These results are quite different with the electron-deficient unit BTD modified porphyrin dyes.[5, 12] It was reported that the dyes (GY50 and SM315) with insertion of BTD between porphyrin chromophore and benzoic acid achieved high efficiency of 13%,[5, 14b] which was superior than the porphyrin (SM371) with benzoic acid acceptor. While connecting porphyrin chromophore to carboxyl acid with BTD, the resulted GY21 porphyrin presented poor PCE of only 4.8%. In this study, the result of LW17, LW18, and LW19 could be used to compare the effect of electron rich units on device photovoltaic parameter. When thiophene was used to connect porphyrin chromophore and carboxylic acid, the resulted LW18 device presents relatively higher J_{SC} values than that of LW17 device. While insertion of a thiophene between the porphyrin chromophore and benzoic acid does not help the improvement of devices performance. These results indicated

that signicant different effects could be achieved whetherever electron-deficient or electron-rich unit was used to modify the porphyrin dyes. The relative high J_{SC} observed in LW18 device might be attibuted to an efficient inner charge transfer from the pyrene-porphyrin conjugate to the carboxylic acid through thiophene.[12] As presented in Fig. 6b, the onset of IPCE responose of LW17, LW18, and LW19 devices stepwise extended from 720 nm, 730 nm, to 740 nm, which were in general agreement with the electronic absorption spectra of dye-sensitized 2.3-μm-thick titania films (see Figure S11). The extended IPCE of LW18 device comparing to LW17 should be account for the higher J_{SC}. It was worthy to note that LW19 devices presented an extended IPCE response compared to other two. Despite of having excellent light-harvesting properties, the LW17-LW19 dyes lack absorption in the 480 to 630 nm range as evidenced by the IPCE spectra in Fig. 6b. The valley in the green spectral region would reduce the device photocurrent and hence the PCE. Co-sensitization is an effective method to avoid this loss, which combines two or more light-harvester with complementary absorption spectra to realize full-spectrum light-harvesting.[29] The V_{OC} of LW18 (700±6 mV) is higher than LW17 (688±10 mV) and LW19 (680±4 mV), which is discussed below.

Table 2 Photovoltaic parameters [a] of porphyrins sensitized solar cells with I^-/I_3^- redox couple (AM 1.5G 96.5 mW cm^{-2}). The cells were measured using a mask (area= 0.09 cm^{-2}).

device	J_{SC} (mA cm^{-2})	V_{OC} (mV)	FF	PCE (%)
LW17	15.67±0.22	688±10	0.72±0.02	7.81±0.28
LW18	17.27±0.26	700±6	0.71±0.02	8.74±0.22
LW19	15.42±0.16	680±4	0.68±0.02	7.26±0.16

[a] The uncertainties represent the standard deviations of the measurements. The photovoltaic parameters are averaged values obtained from analysis of the J-V curves of the identical working electrodes for three devices, fabricated and characterized under the same experimental conditions.

TPD and charge extraction measurements were used to investigate the difference in V_{OC} for DSSCs using the novel porphyrin dyes. Usually, the difference of V_{OC} can original from two major reasons: (i) a shift of the TiO_2 conduction band edge bending with respect to the electrolyte potential, and (ii) difference in the e^--TiO_2/electrolyte$^+$ recombination reaction. The information about conduction band edge shift and the distribution of trap states of TiO_2 could be provided by the chemical capacitance (C_μ).[29b] As shown in Fig. 7a, the C_μ is almost the same for the three devices at a high given voltage, while the slope of capacitance against open circuit voltage for LW17 device is smaller than other two. This result indicates a steeper drop of the density of states below the conduction-band edge in LW17 device. The relationship of electron lifetimes and V_{OC} is plotted in Fig. 7b, affording an insight into the electron recombination occurring at the TiO_2-electrolyte interface. A longer electron lifetime implies a less recombination reaction on the dye-sensitized TiO_2/electrolyte interface.[6a] The LW18 device presented an obviously longer lifetime comparing to LW17 and LW19, indicating a reduced interfacial charge recombination in this device. The device fabricated with LW19 with the longest conjugation length exhibited the shortest electron lifetime. The result could be explained by the reduced molecule dipole moment of LW19 dye. Therefore, the observed photovoltage variation of devices based on these novel porphrins could be principally due to a different charge recombination raction occurring at the dye-sensitized TiO_2-electrolyte interface.

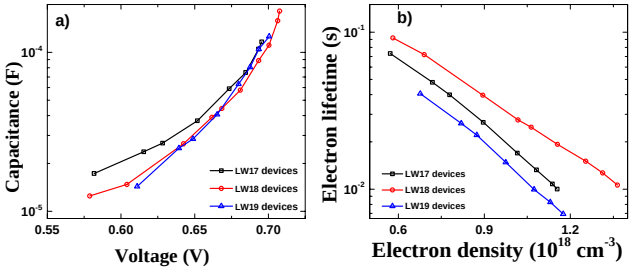

Fig. 7 Transient photovoltage decay and charge extraction measurements of LW17, LW18, and LW19 based DSSC devices. a) Comparisons of electron lifetime at a certain open-circuit photovoltage; b) Comparisons of electron lifetime at a given electron density.

Conclusions

In summary, a series of pyrene-conjugated porphyrin with varies π-spacer have been designed and synthesized for dye-sensitized solar cells. As the π-spacer varied from phenyl (LW17 porphyrin), thiophene (LW18 porphyrin), to 2-phenylthiophene (LW19 porphyrin), the resulted pigments showed stepwise red-shifted absorption spectra and consistently increased oxidation potential. Evaluating these novel dyes with DSSC devices, LW18 with thiophene spacer showed superior power conversion efficiency of 8.7% under full sunlight irradiation, higher than LW17 devices (7.8%) and LW19 devices (7.3%). This work demonstrates that connection porphyrin chromophore and carboxyl acid with electron-rich unit thiophene is beneficial for both photocurrent and photovoltage.

Notes and references

[a] *Wuhan National Laboratory for Optoelectronics, School of Optical and Electronic Information, Huazhong University of Science and Technology, 1037 Luoyu Road, Wuhan 430074 (P. R. China), Fax: (+) 86-27-87792225, E-mail: mingkui.wang@hust.edu.cn*

[b] *College of Materials Science & Engineering, Wuhan Textile University, FangZhi Road, 430073, Wuhan, P. R. China, E-mail: xujie0@mail.ustc.edu.cn*

[c] *Department of Materials Engineering, Monash University, Melbourne,Victoria, 3800, Australia*

† Electronic Supplementary Information (ESI) available: [details of any supplementary information available should be included here]. See DOI: 10.1039/b000000x/

‡ Notes: J. Lu and S. Liu contributed equally.

1 (a) B. O' Regan, M. Grätzel, *Nature*, 1991, **353**, 737–740; (b) S. Kazim, M. K. Nazeeruddin, M. Grätzel, S. Ahmad, *Angew. Chem., Int. Ed.*, 2014, **53**, 2812–2824; (c) P. K. Nayak, D. Cahen, *Adv. Mater.*, 2014, **26**, 1622–1628.

2 (a) C. Y. Chen, M. K. Wang, J. Y. Li, N. Pootrakulchote, L. Alibabaei, C. H. Ngoc-le, J. D. Decoppet, J. H. Tsai, C. Grätzel, C. G. Wu, S. M. Zakeeruddin, M. Grätzel, *ACS Nano,* 2009, **3**, 3103–3109; (b) K. Cao, J. F. Lu, J. Cui, Y. Shen, W. Chen, G. Alemu, Z. Wang, H. L. Yuan, J. Xu, M. K. Wang, Y. B. Cheng, *J. Mater. Chem. A,* 2014, **2**, 4945–4953.

3 (a) A. Mishra, M. K. R. Fischer, P. Bauerle, *Angew. Chem., Int. Ed.*, 2009, **48**, 2474–2499; (b) K. Cao, M. K. Wang, *Front. Optoelectron.* 2013, **6**, 373–385.

4 (a) W. M. Campbell, K. W. Jolley, P. Wagner, K. Wagner, P. J. Walsh, K. C. Gordon, L. Schmidt-Mende, M. K. Nazeeruddin, Q. Wang, M. Grätzel, D. L. Officer, *J. Phys. Chem. C,* 2007, **111**, 11760–11762; (b) I. Hiroshi, T. Umeyama, S. Ito, *Acc. Chem. Res.*, 2009, **42**, 1809–1818; (c) M. J. Griffith, K. Sunahara, P. Wagner, K. Wagner, G. G. Wallace, D. L. Officer, A. Furube, R. Katoh, S. Mori, A. J. Mozer, *Chem. Comm.,* 2012, **48**, 4145–4162; (d) L. L. Li, E. W. G. Diau, *Chem. Soc. Rev.,* 2013, **42**, 291–304.

5 M. Mathew, A. Yella, P.; R. Humphry-Baker, Basile F.E.Curchod, N. Ashari-Astani, I. Tavernelli, U. Rothlisberger, M. K. Nazeeruddin, M. Grätzel, *Nat. Chem.*, 2014, **6**, 242–247.

6 (a) K. Kurotobi, Y. Toude, K. Kawamoto, Y. Fujimori, S. Ito, P. Chabera, V. Sundstrçm, H. Imahori, *Chem. Eur. J.*, 2013, **19**, 17075–17081; (b) J. M. Ball, N. K. S. Davis, J. D. Wilkinson, J. Kirkpatrick, J. Teuscher, R. Gunning, H. L. Anderson, H. J. Snaith, *RSC Adv.*, 2012, **2**, 6846–6853; (c) J. Luo, M. F. Xu, R. Z. Li, K. W. Huang, C. Y. Jiang, Q. B. Qi, W. D. Zeng, J. Zhang, C. Y. Chi, P. Wang, J. S. Wu, *J. Am. Chem. Soc.*, 2014, **136**, 265–272.

7 (a) C. W. Lee, H. P. Lu, C. M. Lan, Y. L. Huang, Y. R. Liang, W. N. Yen, Y. C. Liu, Y. S. Lin, E. W. G. Diau, C. Y. Yeh, *Chem. Eur. J.* 2009, **15**, 1403–1412; (b) T. Bessho, S. Zakeeruddin, C. Y. Yeh, E. W. G. Diau,, M. Grätzel, *Angew. Chem. Int. Edit.*, 2010, **49**, 6646–6649; (c) Y. C. Chang, C. L. Wang, T. Y. Pan, S. H. Hong, C. M. Lan, H. H. Kuo, C. F. Lo, H. Y. Hsu, C. Y. Lin, E. W. G. Diau, *Chem. Commun.*, 2011, **47**, 8910–8912; (d) C. L. Wang, C. M. Lan, S. H. Hong, Y. F. Wang, T. Y. Pan, C. W. Chang, H. H. Kuo, M. Y. Kuo, E. W. G. Diau, C. Y. Lin, *Energy Environ. Sci.*, 2012, **5**, 6933–6940.

8 (a) C. H. Wu, T. Y. Pan, S. H. Hong, C. L. Wang, H. H. Kuo, Y. Y. Chu, E. W. G. Diau, C. Y. Lin. *Chem. Commun*., 2012, **48**, 4329–4331; (b) C. H. Wu, M. C. Chen, P. C. Su, H. H. Kuo, C. L. Wang, C. Y. Lu, C. H. Tsai, C. C. Wu, C. Y. Lin, *J. Mater. Chem. A*, 2014, **2**, 991–999; (c) L. Pellejà, C. V. Kumar, J. N. Clifford, E. Palomares, J. Phys. Chem. C., 2014, DOI: 10.1021/jp411715n; (d) H. Hayashi, A. S. Touchy, Y. Kinjo, K. Kurotobi, Y. Toude, S. Ito, H. Saarenpaa, N. V. Tkachenko, H. Lemmetyinen, H. Imahori, *ChemSusChem*, 2013, **6**, 508–517; (e) Y. Liu, N. Xiang, X. Feng, P. Shen, W. Zhou, C. Weng, B. Zhao, S. Tan, *Chem. Commun.*, 2009, **18**, 2499–2501.

9 C. L. Wang, Y. C. Chang, C. M. Lan, C. F. Lo, E. W. G. Diau C. Y. Lin, *Energy Environ. Sci.*, 2011, **4**, 1788–1795.

10 W. P. Zhou, Z. C. Cao, S. H. Jiang, H. Y. Huang, L. J. Deng, Y. J. Liu, P. Shen, B. Zhao, S. T. Tan, X. X. Zhang, *Org. Electron.*, 2012, **13**, 560.

11 (a) Y. Liu, N. Xiang, X. Feng, P. Shen, W. Zhou, C. Weng, B. Zhao, S. Tan, *Chem. Commun.*, 2009, **18**, 2499–2501; (b) L. Favereau, J. Warnan, F. B. Anne, Y. Pellegrin, E. Blart, D. Jacquemin, F. Odobel, *J. Mater. Chem. A*, 2013, ***1***, 7572–7575; (c) S. Mathew, H. Iijima, Y. Toude, T. Umeyama, Y. Matano, S. Ito, N. V. Tkachenko, H. Lemmetyinen, H. Imahori, *J. Phys. Chem. C*, 2011, **115**, 14415–14424; (d) W. P. Zhou, Z. C. Cao, S. H. Jiang, H. Y. Huang, L. J. Deng, Y. J. Liu, P. Shen, B. Zhao, S. T. Tan, X. X. Zhang, *Org. Electron.*, 2012, **13**, 560–569; (e) E. M. Barea, R. Caballero, L. Lopez-Arroyo, A. Guerrero, P. de la Cruz, F. Langa, J. Bisquert, *ChemPhysChem*, 2011, **12**, 961–965.

12 (a) C. Y. Yi, F. Giordano, N. Cevey-Ha, H. N. Tsao, S. M. Zakeeruddin, M. Grätzel, *ChemSusChem*, 2014. DOI: 10.1002/cssc.201301271; (b) A. Yella, C. L. Mai, S. M. Zakeeruddin, S. N. Chang, C. H. Hsieh, C. Y. Yeh, M. Grätzel, *Angew. Chem., Int. Ed.*, 2014, **126**, 3017–3021.

13 (a) J. F. Lu, X. B. Xu, K. Cao, J. Cui, Y. B. Zhang, Y. Shen, X. B. Shi, L. S. Liao, Y. B. Cheng, M. K. Wang, *J. Mater. Chem. A*, 2013, **1**, 10008–10015; (b) J. F. Lu, B. Y. Zhang, H. L. Yuan, X. B. Xu, K. Cao, J. Cui, S. S. Liu, Y. Shen, Y. B. Cheng, M. K. Wang, *J. Phys. Chem. C*, 2014, **118**, 14739–14748.

14 (a) T. Ripolles-Sanchis, B. C. Guo, H. P. Wu, T. Y. Pan, H. W. Lee, S. R. Raga, F. Fabregat-Santiago, J. Bisquert, C. Y. Yeh, E. W. G. Diau, *Chem. Commun.*, 2012, **48**, 4368–4370; (b) N. M. Reddy, T. Y. Pan, Y. C. Rajan, B. C. Guo, C. M. Lan, E. W. G. Diau D. Y. Yeh, *Phys. Chem. Chem. Phys.*, 2013,**15**, 8409–8415.

15 K. Ladomenou, T. N. Kitsopoulos, G. D. Sharma A. G. Coutsolelos, *RSC Adv.*, 2014, **4**, 21379–21404.

16 (a) H. Imahori, S. Kang, H. Hayashi, M. Haruta, H. Kurata, S. Isoda, S. E. Canton, Y. Infahsaeng, A. Kathiravan, T. Pascher, et al. *J. Phys. Chem. A*, 2011, **115**, 3679–3690; (b) S. Ye, A. Kathiravan, H. Hayashi, Y. J. Tong, Y. Infahsaeng, P. Chabera, T. Pascher, A. P. Yartsev, S. Isoda, H. Imahori, et al. *J. Phys. Chem. C*, 2013, **117**, 6066–6080.

17 B. E. Hardin, H. J. Snaith, M. D. McGehee, *Nat. Photonics*, 2012, **6**, 162–169.

18 J. S. Lindsey, *Acc. Chem. Res.*, 2010, **43**, 300–311.

19 J. F. Lu, X. B. Xu. Z. H. Li, K. Cao, J. Cui, Y. B. Zhang, Y. Shen, Y. Li, J. Zhu, S. Y. Dai, W. Chen, Y. B. Cheng, M. K. Wang, *Chem. Asian J.*, 2013, **8**, 956–962.

20 J. Rochford, D. Chu, A. Hagfelt, E. Galoppini, *J. Am. Chem. Soc.*, 2006, **129**, 4655–4665.

21 M. Gouterman, *J. Chem. Phys.*, 1959, **30**, 1139–1161.

22 S. Verma and H. N. Ghosh, *J. Phys. Chem. Lett.*, 2012, **3**, 1877–1884.

23 A. Hagfeldt, G. Boschloo, L. Sun, L. Kloo, H. Pettersson, *Chem. Rev.*, 2010, **110**, 6595–6663.

24 H. J. Snaith, *Adv. Funct. Mater.*, 2010, **20**, 13–19.

25 J. Warnan, L. Favereau, F. Meslin, M. Severac, E. Blart, Y. Pellegrin, D. Jacquemin, F. Odobel, *Chemsuschem*, 2012, **5**, 1568–1577;

26 (a) N. Santhanamoorthi, C. Lo, J. Jiang, *J. Phys. Chem. Lett.*, 2013, **4**, 524-530; (b) X. Gu and Q. Sun, *Phys. Chem. Chem. Phys.*, 2013, **15**, 15434–15440.

27 (a) S. E. Koops, B. O' Regan, P. R. F. Barnes, J. R. Durrant, *J. Am. Chem. Soc.*, 2009, **131**, 4808–4818; (b) Y. C. Chang, H. P. Wu, N. M. Reddy, H. W. Lee, H. P. Lu, C. Y. Yeh, E. W. G. Diau, *Phys. Chem. Chem. Phys.*, 2013, **15**, 4651–4655; (c) X. Yang, K. Zhang, J. Liu, C. Qin, H. Chen, A. Islama, L. Han, *Energy Environ. Sci.*, 2013, **6**, 3637–3645.

28 (a) J. Bisquert, A. Zaban, M. Greenshtein, I. Mora-Sero, *J. Am. Chem. Soc.*, 2004, **126**, 13550-13559; (b) A. Reynal, A. Forneli, E. Martinez-Ferrero, A. Sanchez-Diaz, A. Vidal-Ferran, B. O'Regan, E. Palomares, *J. Am. Chem. Soc.*, 2008, **130**, 13558–13567; (c) L. L. Li, Y. C. Chang, H. P. Wu, E. W. G. Diau, *Int. Rev. Phys. Chem.*, 2012, **31**, 420–467.

29 a) H.-P. Wu, Z.-W. Ou, T.-Y. Pan, C.-M. Lan, W.-K. Huang, H.-W. Lee, N. M. Reddy, C.-T. Chen, W.-S. Chao, C.-Y. Yeh and E. W.-G. Diau, Energy Environ. Sci., 2012, **5**, 9843–9848; b) A. Yella, H. W.

Lee, H. N. Tsao, C. Y. Yi, A. K. Chandiran, M. K. Nazeeruddin, E. W. G. Diau, C. Y. Yeh, S. M. Zakeeruddin, M. Grätzel, *Science*, 2011, **334**, 629–634.

30 L. Cai, H. Tsao, W. Zhang, L. Wang, Z. Xue, M. Grätzel, B. Liu, *Adv. Energy Mater.* **2013**, 3, 200–205.